

4 EXPERIMENTAL AND NUMERICAL STUDY

4.1 Experimental Study

4.1.1 General

Laboratory model test setups, details of the testing procedure, and numerical modeling of piled raft foundations are presented in this chapter. The experiments were carried out in the Post Graduate Geotechnical Engineering Laboratory of Applied mechanics department, Faculty of Technology and Engineering, The Maharaja Sayajirao University of Baroda. Model tests and their instrumentation were mainly concerned with the contact pressure of model raft, load-settlement characteristics and load sharing mechanism between raft and pile group of model piled raft foundation. The above characteristics were determined by varying the parameters like spacing of piles, L/d ratio of piles, number of piles, shape of rafts, shape of piles, configuration of piles and soil-pile friction. Tests were performed on models of unpiled rafts, single piles, pile groups, and piled rafts.

4.1.2 Factors affecting Experimental Measurements

1) Size of model raft: The size of model raft should be less than $1/5^{\text{th}}$ the size of model test tank so that the lateral expansion of pressure bulb developed during loading stage can remain within the tank. The depth of the sand bed acting as a foundation soil in model tank should be such that the pressure bulb developed in vertical direction during loading stage can remain within the tank. The ultimate bearing/ carrying capacity of sandy soil or cohesion less soil are proportional to the width of footing. Terzaghi suggested that the minimum size of square plate for load test should be 30 cm for reliable results. However many researchers have adopted quite smaller than 30 cm size plate as foundation for model experimental study Beren Yilmaz (2010), Giretti (2010), Mosa et al. (2011). Here for considering the boundary limit of modal tank, the size of model rafts was adopted as 22 cm to 24 cm.

2) Rigidity of raft: The model raft should meet the criteria for rigid raft so that the settlement beneath raft can be considered uniform. Square steel plates with 220 mm side (B_r) and 25 mm thickness (t_r) were used to simulate the model rigid rafts. The raft-soil stiffness ratio (K_{rS})

Experimental and Numerical Study

was calculated by Equation (4-1) to confirm the rigidity of the raft ($K_{rs} \gg 5$) based on the suggestions of Horikoshi and Randolph.

$$K_{rs} = \frac{E_r}{E_s} \left(\frac{1 - \mu_s^2}{1 - \mu_r^2} \right) \left(\frac{t_r}{B_r/2} \right)^3 \quad (4-1)$$

Where E_r the modulus of elasticity of steel is plate (2.1×10^5 MPa), E_s is the soil modulus (21.67 MPa, 33.89 MPa, 39.17 MPa for orsang sand at 40%, 60% and 80% relative density respectively and 13.88 MPa, 20.95 MPa, 25.23 MPa for Narmada sand at 40%, 60% and 80% relative density respectively), B_r is the raft width (0.22 m), t_r is the raft thickness (0.025 m), μ_s is the soil Poisson's ratio calculated using equation(4-2) (0.319, 0.298, 0.27 at 40%, 60% and 80% relative density respectively) and μ_r is the steel Poisson's ratio (0.3). In the present study the minimum value of K_{rs} was 64 and hence rafts were considered to be rigid.

3) Size of model pile: As suggested by DRC committee member Prof. (Dr.) Amit Prashant, Size of the foundation member (model pile) should be minimum 20 times the mean diameter (D_{50}) of foundation sand so as particle size does not affect the results of model load test. Therefore, the diameter of model pile was kept as 9.7 mm which is equal to ($d/D_{50} = 9.7/0.5 \approx 20$).

4) Pile Connection: The connection between piles and raft should be rigid enough so that the raft and piles of piled raft can act as a single unit (structure). If the connection between piles and raft is not rigid enough then there is a chance of disconnection between piles and raft during the loading stage and it may mislead the readings for load carrying and sharing capacity of piled raft foundation. The piles on its top have internal threads that were inserted in the small groove beneath the raft and fixed with the raft from the top by screwing with the Allen bolt, which was flush with the top surface of the raft and gives a rigid connection, hence there is no possibility of connection failure of the pile with the raft (Figure 4-1, Figure 4-2, Figure 4-3, Figure 4-4)

Experimental and Numerical Study



Figure 4-1 : Model pile

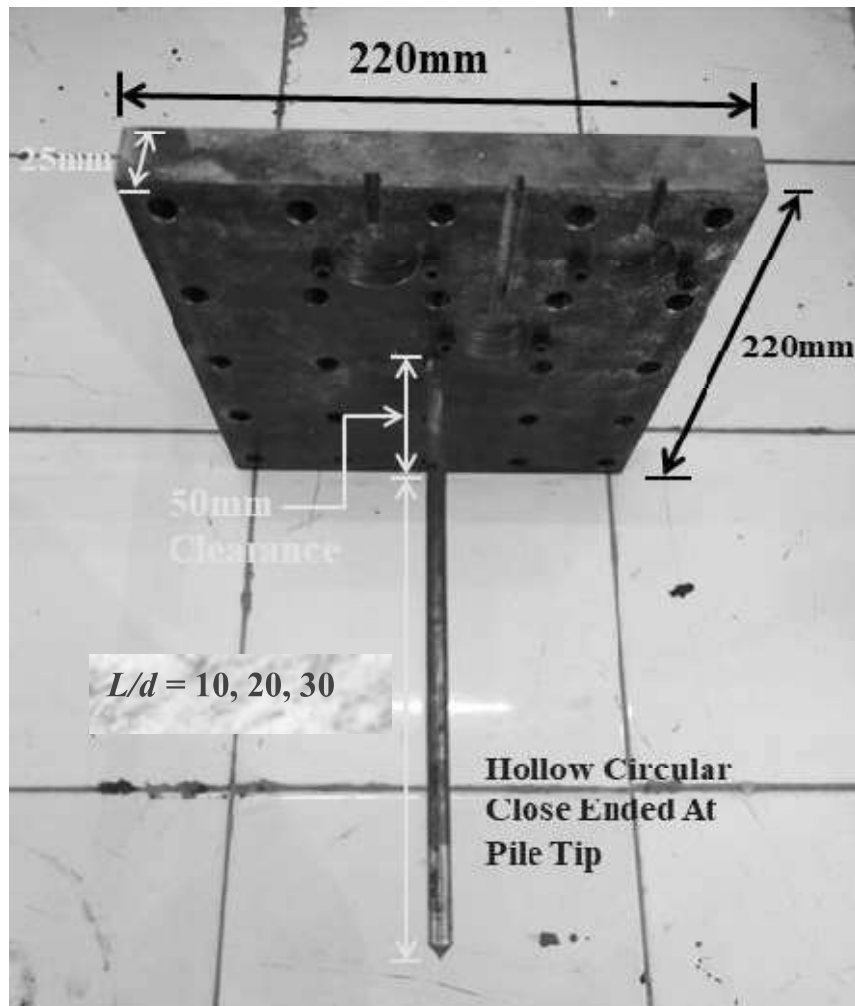


Figure 4-2 : Connection of central pile with raft

Experimental and Numerical Study



Figure 4-3 : Model piled raft foundation



Figure 4-4 : Model pile group

Experimental and Numerical Study

5) Eccentricity of load: Present study is directed toward the concentric load application to UPR, PG and PRF. If the load is eccentric then there will be tilting of raft which leads differential settlement and changes the load sharing mechanism. Hence care was taken to apply the load as far as possible concentric and in vertical direction. The raft was placed on a leveled foundation sand bed and it was leveled using leveling tube. It was aligned centrally in the tank and located axially below the mechanical screw jack and proving ring with the use of plumb bob so that the top C.G of the raft aligned vertically with the axis of screw jack and proving ring (Figure 4-5).



Figure 4-5 : centering of model piled raft using plumb bob

6) Raft- soil, Pile-soil interaction:

The interaction between raft, piles and piled raft foundation along with soil-structure interaction play important role on bearing capacity, settlement characteristics, raft forces and contact pressure distribution, pile forces and pile displacement along with soil reaction on it. The stiffness and deformation characteristics of the soil and the raft affect the transfer of loads between them. The flexibility of the raft and the stiffness of the soil play a significant role in determining the stress distribution and settlement behaviour. Since it is the heart of thesis, it is discussed fully in chapter 5.

Experimental and Numerical Study

7) Preparation of foundation bed: The foundation sand bed should be prepared in accordance with desired relative density. The relative density should be reproducible according to the requirement of test on same density. In this study for achieving desired density of sand bed various trials were made to compact the sand in layers using surface vibrator. The thickness of layer and duration of vibration were finalized from the trials, the details of which are given in Table 4-6. Wooden boxes and steel boxes were placed at different layer of sand bed at the time of preparing sand bed for experiments to check whether the desired density was achieved or not.

8) Rigidity of model tank and load frame: The rigidity of model tank and load frame should be such that load on the raft/ piled raft can be distributed evenly in the soil. The strong load frame was fabricated from double c section and angle sections and the tank bottom was made enough strong with angle stiffeners so that load on the raft/ piled raft can be distributed evenly in the soil.

9) Interpretation of test results: Several factors influence pile load test interpretation, including soil-pile interaction, soil variability, pile installation impacts, load test method, failure mode, and analysis method. For example, interpreting pile load tests in cohesive soils may necessitate taking into consideration time-dependent factors like as consolidation, creep, and relaxation. Non-linear effects such as densification, dilatation, and plugging may need to be considered when interpreting pile load testing in granular soils.

In the static pile load test, the ultimate capacity is defined as when a rapid movement occurs under constant or slightly increased load. Because of large movements required for a pile to reach plunging mode failure, on most occasions a distinct plunging ultimate load is not obtained in the test (Fellenius and Tech, 2001). Therefore, several interpretation criteria have been proposed and are applied for determining the pile ultimate capacity. It is necessary to apply a unique failure criterion in defining the ultimate capacity to make the load test results comparable. Six failure criteria have been summarized by Fellenius (1980). Among these approaches, the Davisson offset limit (Davisson, 1972), the Brinch-Hansen 80% criterion (Brinch Hansen, 1963) and the Chin-Kondner extrapolation (Chin, 1978) are commonly used (Figure 4-6). The Davisson limit load usually reports loads in the lower part of the load-displacement diagram. On the other hand, the Chin-Kondner extrapolation assumes an

Experimental and Numerical Study

asymptotic curve and the load are defined by extrapolation, and therefore, the results are always greater than the maximum load applied in the test. The Brinch-Hansen 80% criterion normally agrees well with the intuitively perceived “plunging failure” of the pile (Fellenius and Tech, 2001). In this study Davisson method is used for defining the ultimate capacity of piles. In the present investigation, the load-settlement curve indicates initial straight line reaching to convex upward to the point from where it falls into straight line with progressive high settlement that point is taken as ultimate load of the pile / pile groups. In some of the cases, the load at settlement = 10% of diameter of pile is considered as failure load for single pile (Figure 4-6).

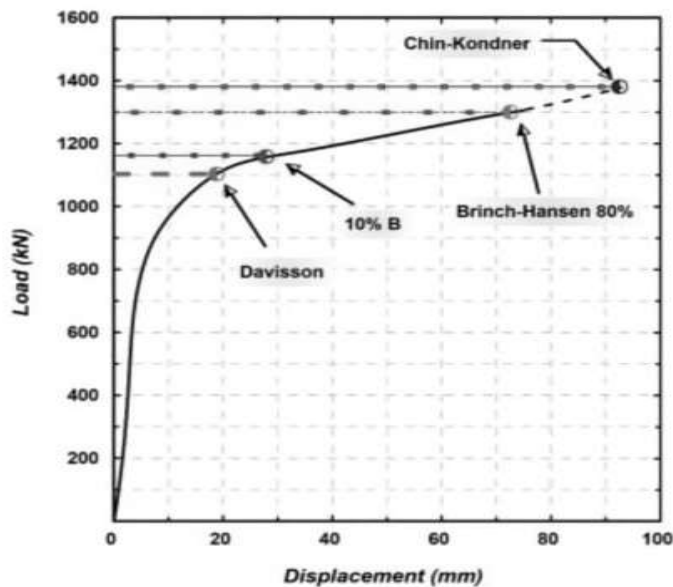


Figure 4-6 : Interpretation of load-displacement diagram (after Moshfeghi and Eslami, 2016)

4.1.3 Model Pile/ Pile Group

Mild Steel rods with hollow circular cross section having 9.7 mm external diameter, 0.95 mm thickness and length to external diameter (L/d) ratios 10, 20, 30 were used as a model piles (Table 4-1). The bottom part of pile was closed cone having 120° internal angle. Threads were provided at the top end of inner side of piles to fix with raft using screw from the top of the raft for generating monolithic action between the piles and the raft. For test on free

Experimental and Numerical Study

standing pile groups a set of piles were made 50 mm longer than the piles of piled raft (Figure 4-1, Figure 4-7, and Figure 4-8).

Table 4-1 Dimensions of Hollow piles with closed cone end

| | |
|--|-------------|
| External Diameter of piles (d) in mm | 9.7 |
| Internal Diameter of piles (d_i) in mm | 7.8 |
| Total length of piles (L_t) in mm for free standing pile group | 157,254,351 |
| Embedded length of piles (L) in mm | 97,194,291 |
| L/d ratio | 10,20,30 |

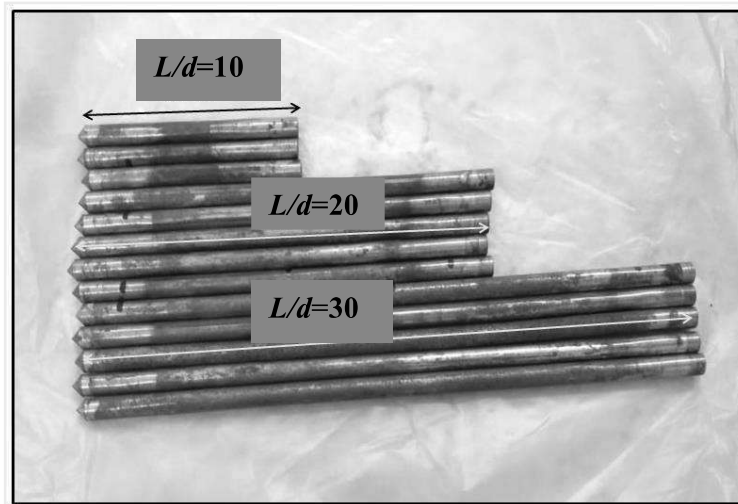


Figure 4-7 : Model piles with different L/d ratio of piles

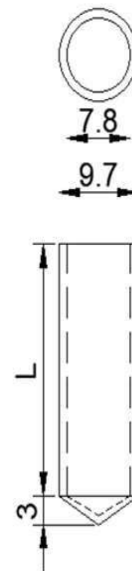


Figure 4-8 : Schematic diagram of Model piles (Hollow circular cross section with close end)

The dimensions of piles used for the study of different shape of piles are as listed in Table 4-2 and shown in Figure 4-9 to Figure 4-10.

Experimental and Numerical Study

Table 4-2 Dimensions of piles used for the study of different shape of piles

| Shape of piles | Dimensions | | | | Cross sectional Area |
|----------------------|-----------------------|----------------------|-------------------------|----------------------|-----------------------|
| Hollow Circular (HC) | Outer Diameter- 16 mm | Inner diameter-12 mm | | | 87.96 mm ² |
| H- pile | Flange width - 15 mm | Web height - 14 mm | Flange thickness - 2 mm | Web thickness - 2 mm | 88 mm ² |
| Hollow Square (HSQ) | Side - 16 mm | Thickness - 1.5 mm | | | 88 mm ² |

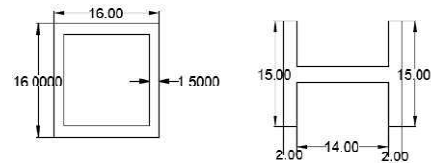
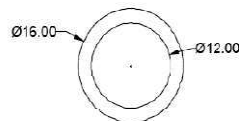


Figure 4-9 : Model piles with different shape of piles

Figure 4-10 : Schematic diagram of cross section of Model piles with different shapes

To study the effect of soil-pile friction on load carrying capacity of piled raft foundation, the piles were prepared with different degree of friction on surface of pile (achieved by fixing different size of sand particles on pile surface). Different surface roughness of pile surface was achieved by pasting the different size of sand particle on pile surface with the help of strong epoxy adhesive with a 17 MPa lap shear strength to produce a certain level of pile surface roughness. Three types of specific sand particles sieved from Badarpur sand (Orsang river sand) which were passing 212 μm sieve and retained on 75 μm , another sand passing 425 μm sieve and retained on 212 μm , and the third one passing 600 μm sieve and retained

Experimental and Numerical Study

on 425 μm , were fixed on the pile outer surface evenly using strong epoxy adhesive to achieve different degree of pile roughness. This study was made for pile with L/d ratio = 30.

The direct shear box tests were performed for finding out the soil-pile friction angle at different relative density of natural Badarpur sand. The same sands discussed in earlier paragraph were fixed on mild steel plates to determine soil-pile interface friction angle as shown in Figure 4-11 and obtained values are displayed in table Table 4-3 and Table 4-4...

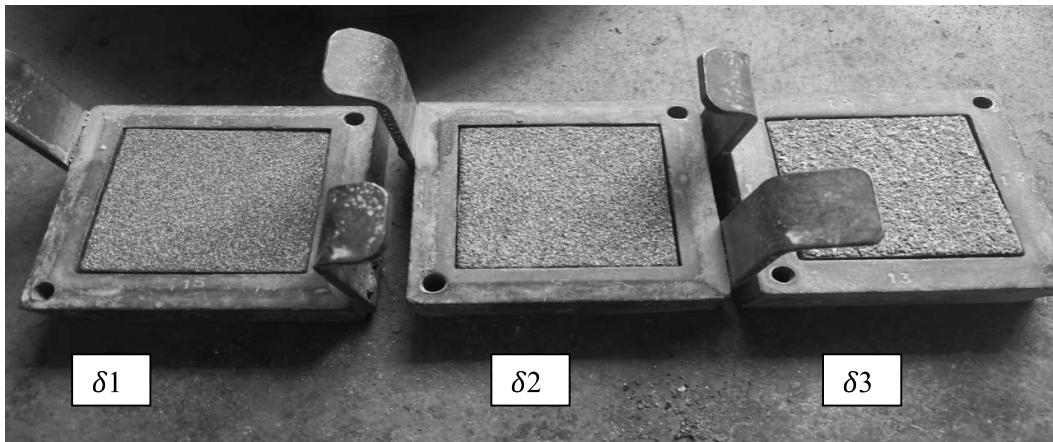


Figure 4-11 : Mild steel Plate with different roughness used in direct shear box test to measure the different soil pile friction angle

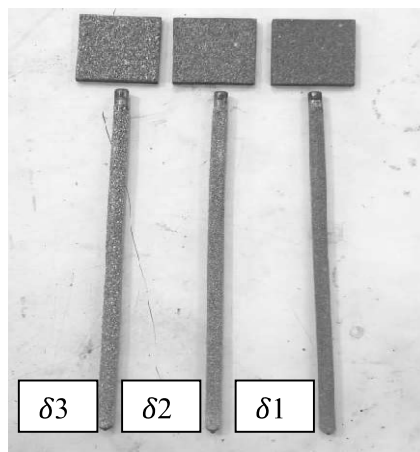


Figure 4-12 : Mild steel Plate and model piles with different roughness or soil pile friction angle

Experimental and Numerical Study

Table 4-3 Notations of different soil-pile friction angles based on the degree of pile surface roughness

| Sr.No. | Notations (soil-pile friction angle) | Description of interface friction angle |
|--------|---|--|
| 1 | δ_0 | Plain mild steel surface and natural Badarpur sand |
| 2 | δ_1 | Mild steel surface fixed with sand particles passing 212 μm sieve retained on 75 μm and natural Badarpur sand |
| 3 | δ_2 | Mild steel surface fixed with sand particles passing 425 μm sieve and retained on 212 μm and natural Badarpur sand |
| 4 | δ_3 | Mild steel surface fixed with sand particles passing 600 μm sieve and retained on 425 μm and natural Badarpur sand |

4.1.4 Model Raft

Mild steel plates were used to prepare the model rigid rafts. The dimensions of model rafts with different shapes are as shown in Table 4-5. Figure 4-13 to Figure 4-21 show the detailed dimensions of model raft with the arrangement of earth pressure cells (EPC) and piles. Small circle having 10 mm diameter and big circle having 31 mm diameter in Figure 4-13 to Figure 4-21 display the position of piles and EPC in PRF respectively.

Experimental and Numerical Study

Table 4-4 soil-pile friction angles obtained from direct shear box test

| Sr. No | Relative Density (I_d) | Unit Weight gm/cc | Direct Shear Box Test Data | | |
|--------|----------------------------|-------------------|---|--------------------------------------|------------------------------------|
| | | | Angle of shear resistance of soil (degrees) | Notations (soil-pile friction angle) | Soil pile friction angle (degrees) |
| 1 | 40% | 1.62 | 32.58 | δ_0 | 22.55 |
| | | | | δ_1 | 24.36 |
| | | | | δ_2 | 25.80 |
| | | | | δ_3 | 27.10 |
| 2 | 60% | 1.68 | 34.89 | δ_0 | 24.50 |
| | | | | δ_1 | 25.70 |
| | | | | δ_2 | 26.58 |
| | | | | δ_3 | 28.62 |
| 3 | 80% | 1.75 | 37.16 | δ_0 | 26.30 |
| | | | | δ_1 | 27.41 |
| | | | | δ_2 | 28.22 |
| | | | | δ_3 | 30.04 |

Table 4-5 Dimensions of different shape of model raft

| Shape of model raft | Plan dimensions (mm) | Thickness (mm) |
|---------------------|--|----------------|
| Square | 220 x 220 | 25 |
| Square | 240 x 240 | 25 |
| Circular | 248.24 (Dia.) | 25 |
| Rectangular | 260 x 186.1 | 25 |
| Trapezoidal | Long side = 240 | 25 |
| | Short side = 180 | |
| | Perpendicular distance between short and long side = 230 | |

Experimental and Numerical Study

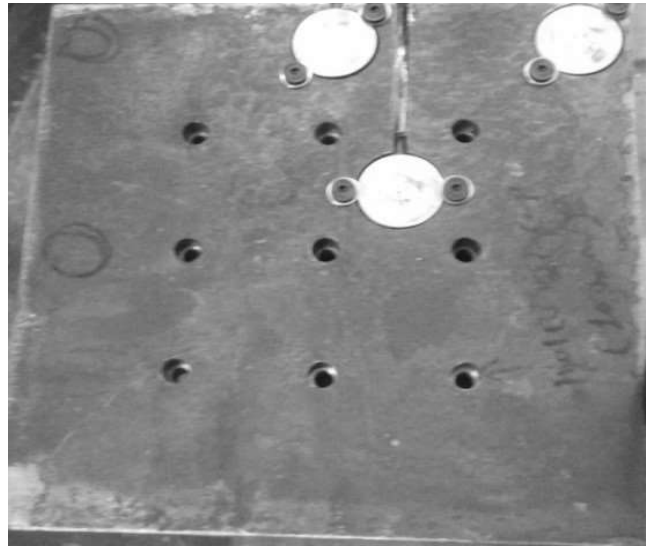
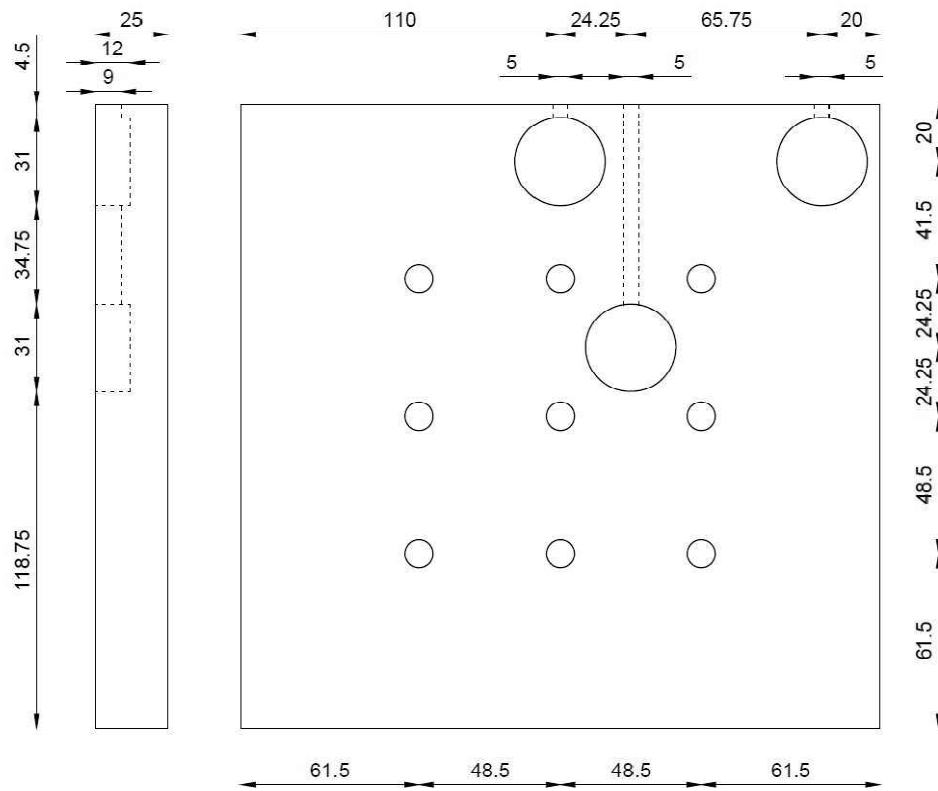


Figure 4-14 : Model raft of piled raft foundation with spacing between piles = $5d$
 (Shape of raft = Square; $S = 5d$; PG = 3×3 ; All dimensions in mm)

Experimental and Numerical Study

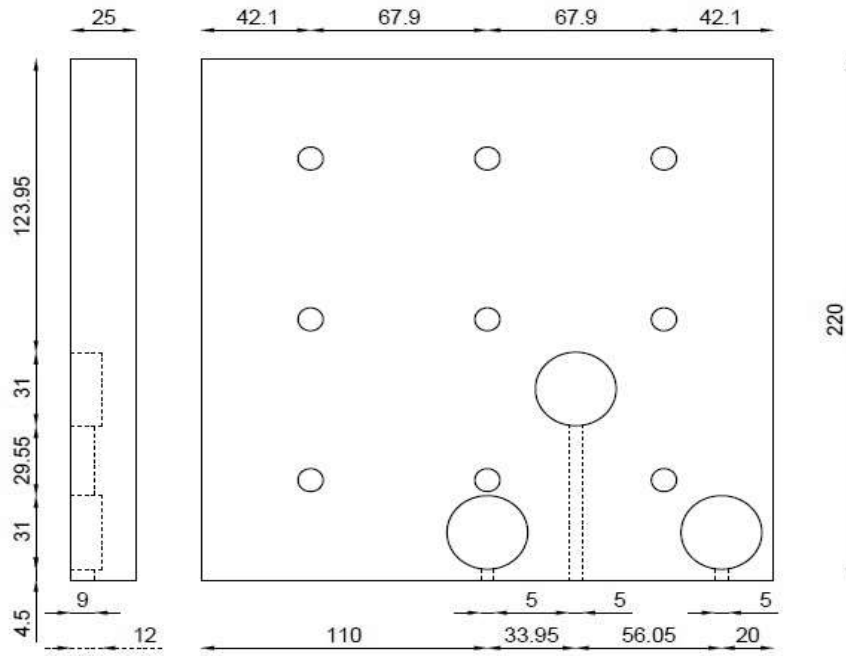


Figure 4-15 : Model raft of piled raft foundation with spacing between piles = $7d$
 (Shape of raft = Square; $S = 7d$; PG = 3×3 ; All dimensions in mm)

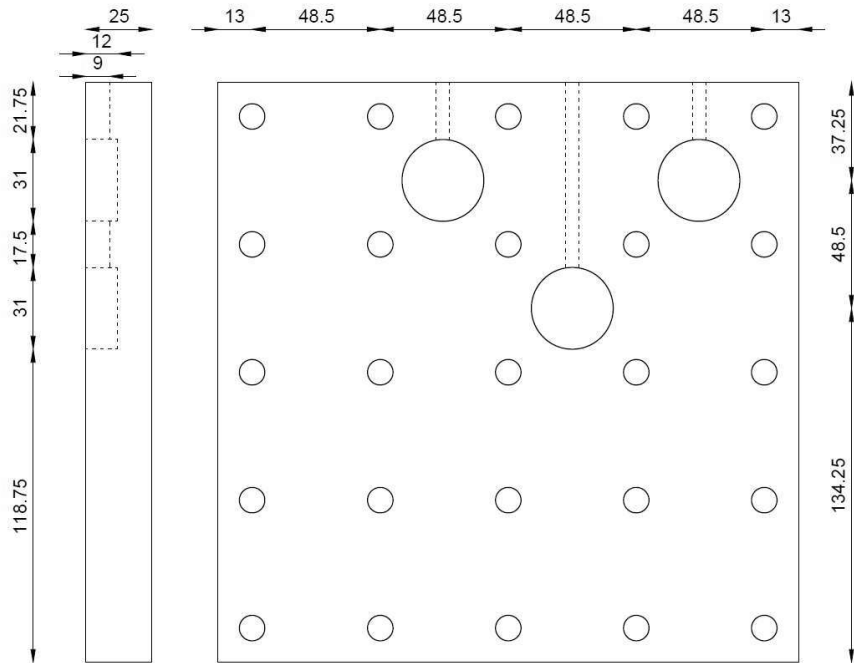


Figure 4-16 : Model raft of piled raft foundation with different L/d ratio of piles
 (Shape of raft = Square; $S = 5d$; PG = 3×3 ; $L/d = 10, 20, 30$; All dimensions in mm)

Experimental and Numerical Study

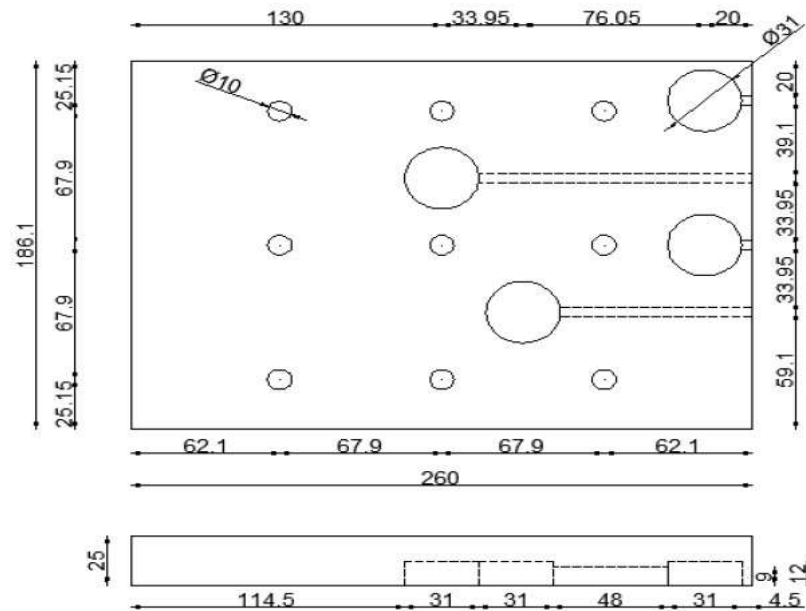


Figure 4-17 : Model raft of piled raft foundation with rectangular raft (Shape of raft = rectangular; $S = 7d$; $PG = 3 \times 3$; $L/d = 30$; All dimensions in mm)

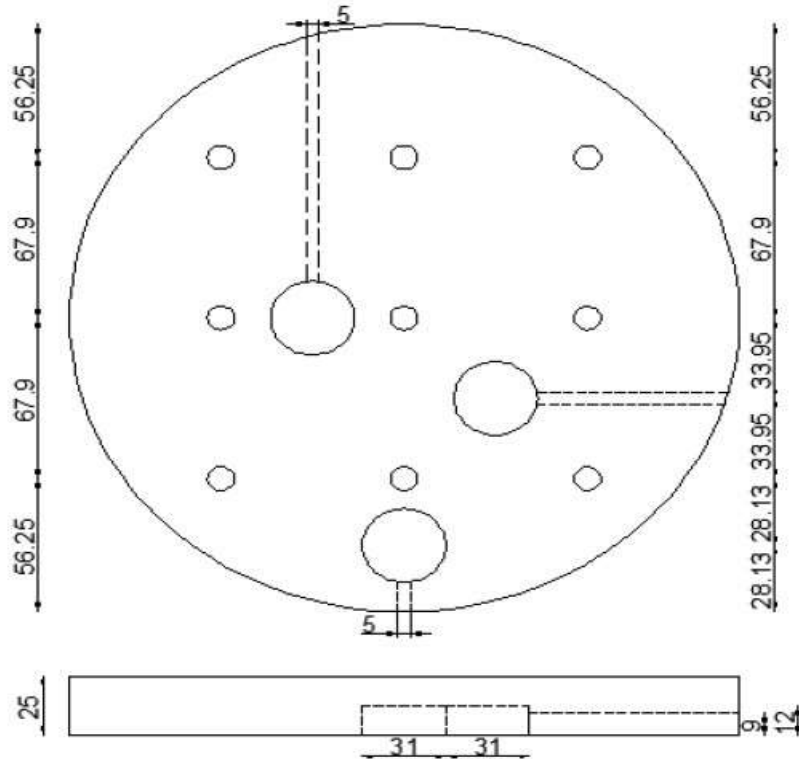


Figure 4-18 : Model raft of piled raft foundation with circular raft (Shape of raft = circular; $S = 7d$; $PG = 3 \times 3$; $L/d = 30$; All dimensions in mm)

Experimental and Numerical Study

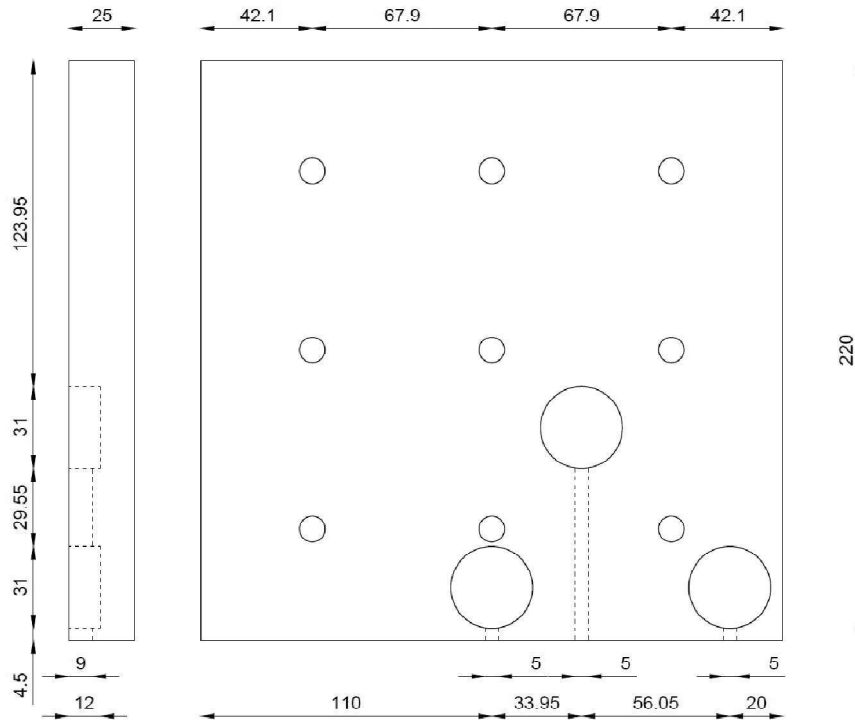


Figure 4-19 : Model raft of piled raft foundation with square raft (Shape of raft = square; $S = 7d$; $PG = 3 \times 3$; $L/d = 30$; All dimensions in mm)

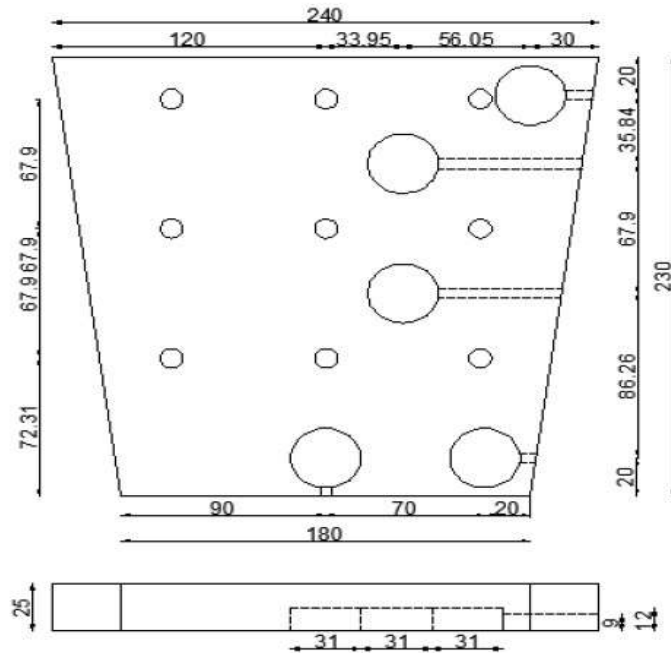


Figure 4-20 : Model raft of piled raft foundation with trapezoidal raft (Shape of raft = trapezoidal; $S = 7d$; $PG = 3 \times 3$; $L/d = 30$; All dimensions in mm)

Experimental and Numerical Study

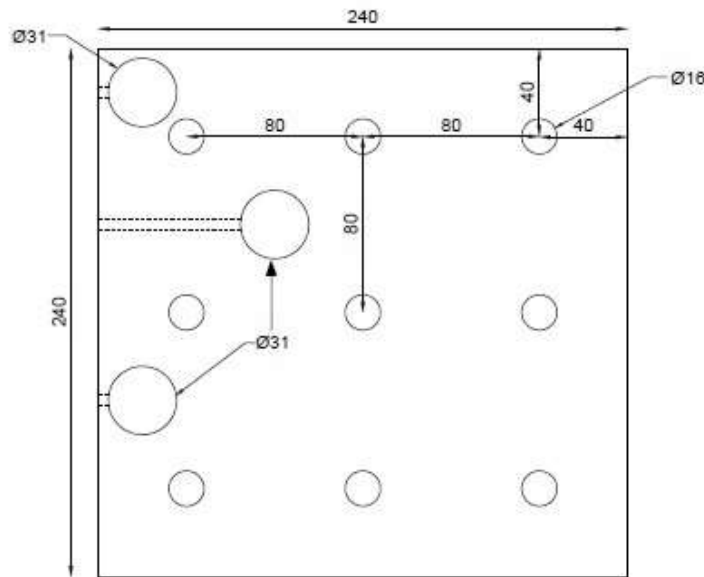


Figure 4-21 : Model raft of piled raft foundation with different shape of piles (Shape of raft = square; $S = 5d$; $PG = 3 \times 3$; $L = 300$ mm; All dimensions in mm)

4.1.5 Model Piled raft

Model piled raft consist model raft as well as model piles as a component of model piled raft foundation. The model raft and piles described in above sections were used to prepare model piled raft foundation. Based on the parameters considered in this study the model piled rafts were prepared as below:

(i) Shape of raft: For studying the effect of shape of raft on behaviour of model piled raft, four model piled rafts were prepared using four shapes of raft (square, circular, rectangular, and trapezoidal) with equal contact area and nine piles ($L/d = 30$) in square group.

(ii) L/d ratio of piles: To study the effect of L/d ratio of piles on behaviour of model piled raft, three model piled rafts were made using square raft and twenty five piles in each model piled raft with $5d$ spacing and $L/d = 10$, $L/d = 20$ and $L/d = 30$ in a 5×5 pile group.

Experimental and Numerical Study

(iii) Spacing between piles: To study the effect of spacing between piles on behaviour of model piled raft foundation, three model piled rafts were prepared by using square model raft and nine piles of $L/d = 30$ in a square group with $3d$, $5d$, and $7d$ c/c spacing between piles.

(iv) Configuration of piles: There were nine configurations of piles in model piled raft studied by varying the length and position of piles in a 5×5 pile group with $5d$ spacing as shown in Figure 4-22. The effect of configurations on behaviour of piled raft foundation was studied at 60% relative density of sand bed. The abbreviation used for different piles are : long piles (LP); medium piles (MP); short pile (SP) and for configuration it is CF.

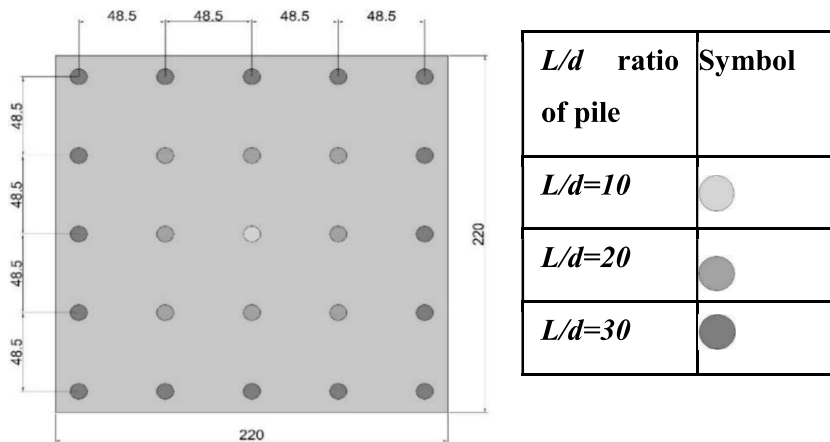


Figure 4-22 : Model piled raft for the study of configuration of piles (All dimensions are in mm)

Experimental and Numerical Study

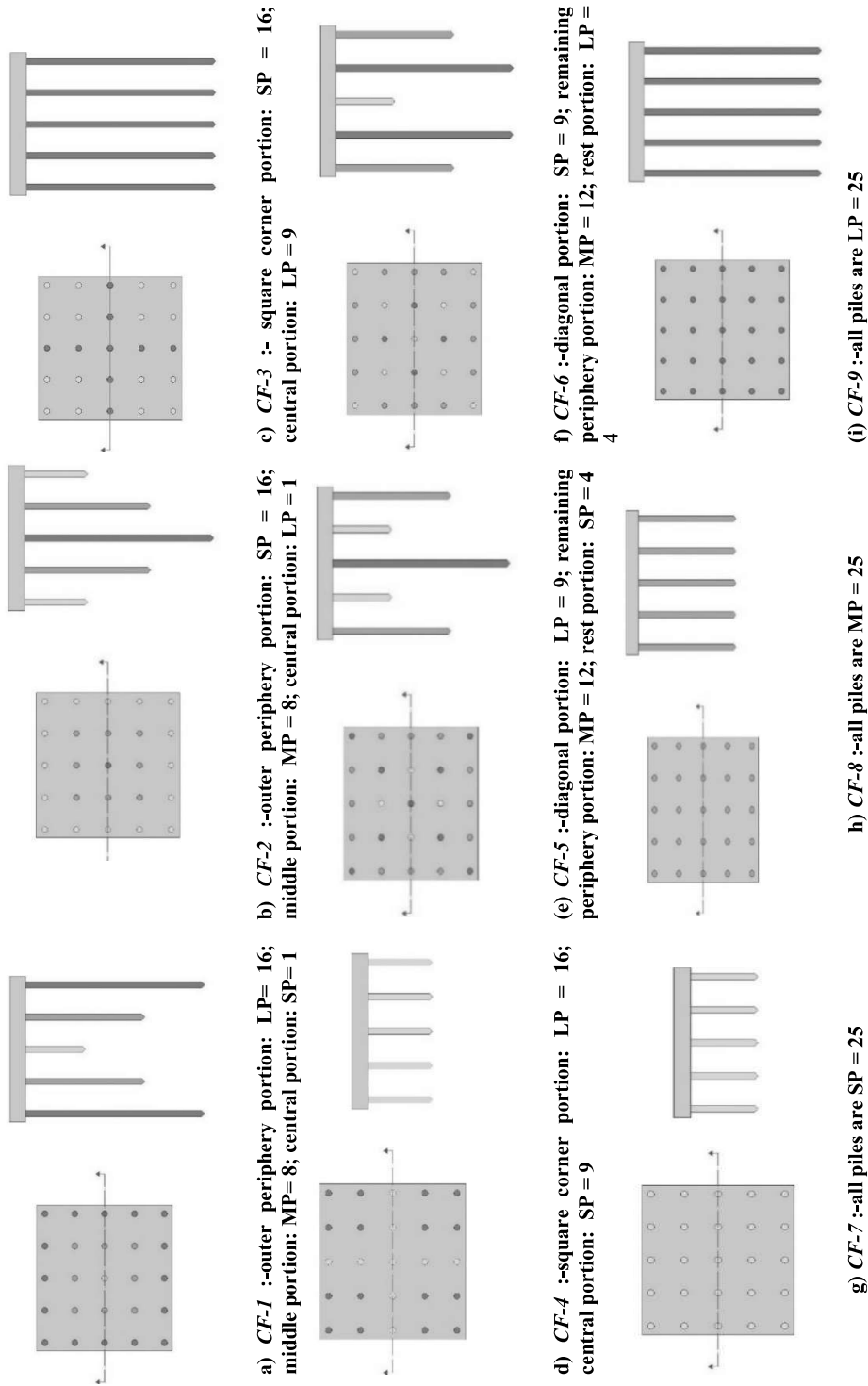


Figure 4-23 : Configuration of pile with varying length of piles and position of pile

Experimental and Numerical Study

v) **soil-pile friction angle:** The effect of soil-pile friction angle on behaviour of model piled raft foundations were studied with 3×3 pile group keeping spacing between piles as $5d$, and L/d of piles as 30. There were 4 model piled raft prepared with square raft and nine piles in a square group with four different soil-pile friction angles (δ_0 to δ_3) as mentioned in Table 4-4 and tested on sand bed with 40%, 60% and 80% relative density.

vi) **shape of piles:** There were three model piled raft made by using square raft and nine piles of length 300 mm with H, hollow circular and hollow square cross sections of equal area in 3×3 pile group keeping spacing between piles as $5d$. These model piled raft were tested on Narmada river sand bed with 40%, 60% and 80% relative density.

4.1.6 Model Tank and Loading Frame

The model tests were performed in a tank measured 1200 mm×1200 mm in plan and 1070 mm in depth and was made of mild steel plate, one side Perspex sheet and angle stiffeners. The tank bottom was made enough strong by stiffeners and supported by a reaction loading frame constructed of channel and angle sections. The mechanical screw jack was attached centrally on the top of the reaction frame, as shown in Figure 4-24. A proving ring was held between the raft and the mechanical screw jack to measure the load. The tank's total height was divided into 50 mm intervals.

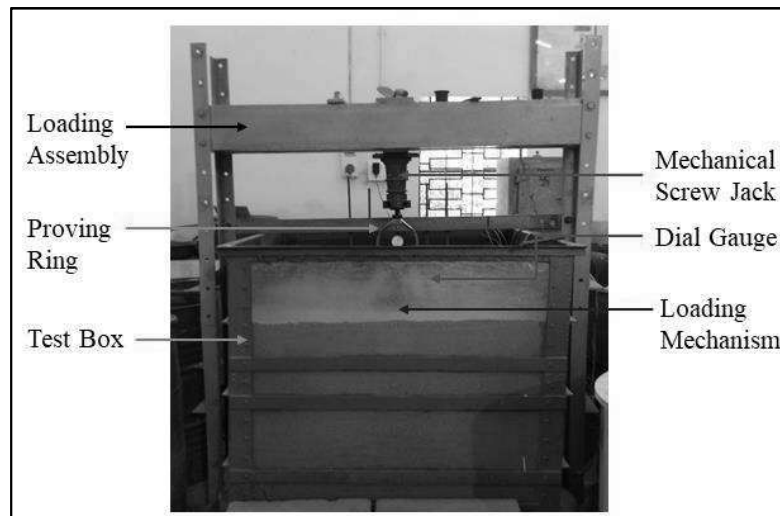


Figure 4-24 : Experimental set-up

Experimental and Numerical Study

4.1.7 Surface Vibrator for Compaction of Sand

The dimensions, weight, and frequency of surface vibrator used for compaction of sand were 320 mm × 310 mm, 16.9 kg, and 1400 rpm, respectively (Figure 4-25). The motor of vibrator was operated on 220-230V A.C. supply.

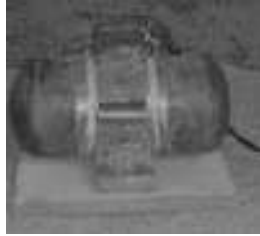


Figure 4-25 : Surface vibrator

4.1.8 Mild Steel Compaction Frame and Rammer

For compaction in the central portion of the piled raft, mild steel compaction frame (Figure 4-28) and rammer were used. The model piled raft was placed with the mild steel compaction frame at desired level as shown in Figure 4-29. The sand between piles was compacted by tamping on frame with standard proctor rammer to achieve the desired density. After compacting top most layer of sand, raft and mild steel compaction frame was removed from the top by unscrewing and raft was reconnected again with piles as shown in (Figure 4-29 to Figure 4-32). The confirmation of the desired density achievement was done using galvanized steel density boxes (Figure 4-26, Figure 4-27).

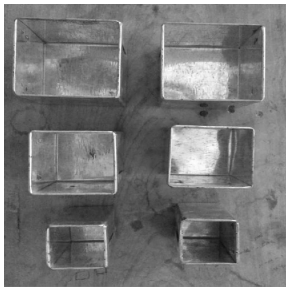


Figure 4-26 : Galvanized steel boxes

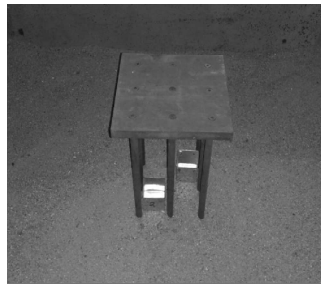


Figure 4-27 : Arrangement of density box between piles

Experimental and Numerical Study



Figure 4-28 : Compaction frame



Figure 4-29 : Mild steel compaction frame for compacting the soil between the piles



Figure 4-30 : Removal of compaction frame after compacting the soil between the piles at topmost layer

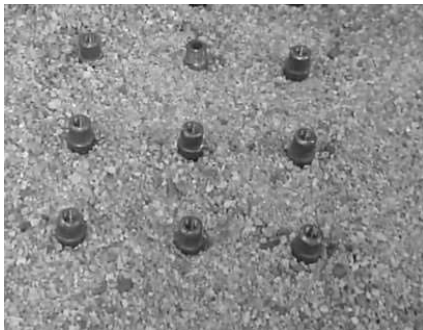


Figure 4-31 : Removal of raft and compaction frame after compacting the soil between the piles at topmost layer

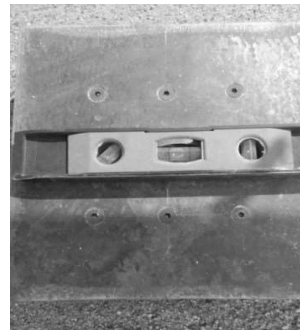


Figure 4-32 : Reconnection of raft with frame after compacting the soil between the piles

4.1.9 Instrumentation

The instrumentation was done for measuring load, settlement and contact pressure beneath model raft foundation.

Experimental and Numerical Study

- a) Proving ring: Proving ring of capacity 250 kg, 10 kN, 25 kN, and 50 kN calibrated from HEICO company, New Delhi were used to measure load.
- b) LVDT: Calibrated Linear variable Displacement Transducers were used to measure the settlement of the model foundations at different load level. The maximum measuring capacity of the LVDT was 100 mm with 0.01 mm accuracy.
- c) Dial gauges: Calibrated Dial gauges were used to measure the settlement of the model foundations at different load level. The maximum measuring capacity of the Dial gauges was 50 mm with 0.01 mm accuracy.
- d) Earth Pressure Cells and its indicator: Calibrated Earth Pressure Cells (EPC) from M/s NICTECH, Jaipur and checked in our department were used to measure the contact pressure beneath the raft at soil interface at critical location. The usual and rated maximum measuring capacity of the EPC were 750 kPa and 1400 kPa, respectively with 1 kPa least count (Figure 4-33). The readings of EPC were observed from the indicator of EPC (Figure 4-34). Earth pressure cells (EPC) were placed in the groves at the bottom of the raft in such a way that the bottom surface of the raft and the bottom surface of EPC met in a plane, as shown in the Figure 4-14, to investigate the contact pressure distribution between the raft and the soil. The earth pressure cells were 30 mm in diameter and 12 mm in thickness.
- d) Strain gauges and its indicator: Strain gauges were used to measure the axial strain developed in the piles at different load level. The readings of Strain gauges were observed from the indicator of strain gauge (Figure 4-34).

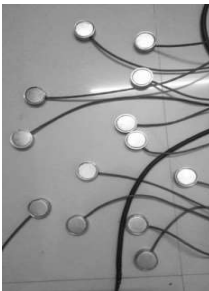


Figure 4-33 : Earth pressure cells
Figure 4-34 : Indicator of earth pressure cells and strain gauges

Experimental and Numerical Study

4.1.10 Preparation of Foundation Soil (sand bed) and Installation of Foundation Test Setup (UPR, PG, PRF)

The desired relative densities of Orsang River's sand were achieved by taking 20 trial tests on various thickness of sand layer and various duration of vibration on each layer. The inner side of tank was marked at interval of 5 cm from bottom to top as shown in Figure 4-35. The tank was filled with sand in layer wise and the thickness of layer was varied from 5 cm to 15 cm and vibration was applied with surface vibrator on this layer for 30sec, 45 sec, 1 min, 1.5min, 2 min, 2.5 min, 3min, 3.5 min, 4 min, 4.5 min, 5 min, 5.5 min, 6 min, 6.5min and 7 minutes. Rigid wooden boxes and metal boxes were used to measure density of sand after vibration. Wooden boxes of size 15 cm × 10 cm × 7.5 cm, 10 cm × 10 cm × 7.5 cm, and metal boxes of size 5.4 cm × 5.4 cm × 4.5 cm, 4.4 cm × 4.4 cm × 4.5 cm, and 1.5 cm × 5 cm × 4 cm were used depending on the thickness of layer tried as shown in Figure 4-36. The results of achieved desired relative densities are shown in Table 4-6. Some of these boxes were kept in the different layers during actual performance of load test to countercheck the density of sand bed.

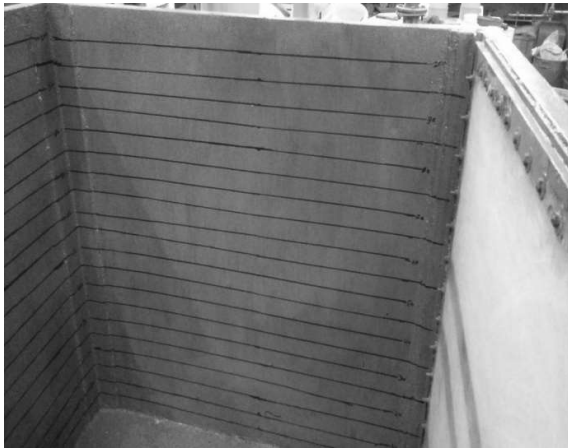


Figure 4-35 : Marking at every 5 cm height on inner side of tank

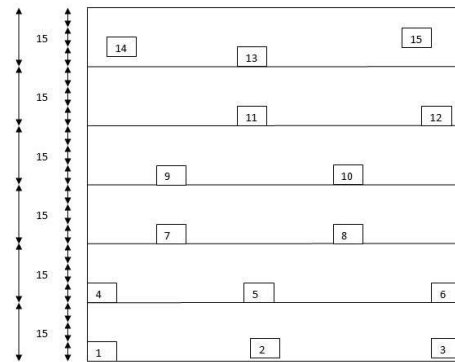


Figure 4-36 : Arrangement of boxes for the determination of densities

Experimental and Numerical Study

Table 4-6 Details of parameters used to achieve the desired density of sand using surface vibration technique

| Type of Sand | Density (gm/cm ³) | Relative Density (%) | Thickness of Layer (mm) | Duration of Vibration (sec) |
|--------------|-------------------------------|----------------------|-------------------------|-----------------------------|
| Orsang | 1.62 | 40 | 150 | 45 |
| | 1.68 | 60 | 100 | 85 |
| | 1.75 | 80 | 50 | 60 |
| Narmada | 1.52 | 40 | 100 | 30 |
| | 1.57 | 60 | 100 | 60 |
| | 1.62 | 80 | 50 | 90 |

4.1.11 Test Procedure

The test procedure consisted of the following steps:

1. The tank's total height was divided into 50 mm intervals. The sand was filled in the tank in layers and vibrated with surface vibrator for specific time to achieve desired relative density, the details of which are given in Table 4-6.
2. The sand was filled in layers in the tank until it reached 55 cm / 60cm thickness from bottom of tank. The model piled raft was put on this compacted sand bed in such a way that centre of gravity of the raft aligned with the centre of the mechanical screw jack using a plumb bob and raft was levelled with a spirit level. Piled raft was driven 5cm into sand bed from its previous position by pressing it with the mechanical screw jack. The sand in the periphery of the piled raft was poured with predetermined height of 15 cm and vibrated with surface vibrator for the next layer. For compaction in the central portion of the piled raft, raft was removed from the top by unscrewing and sand was poured from 15 cm height in between the piles. The piles were inserted in the holes of the bottom plate of the compaction frame and raft was reattached with piles. The sand between piles was compacted with this frame by applying predetermined blows of standard proctor rammer and this procedure was repeated up to top layer. After compacting top most layer (up to 80 cm from bottom of tank) the

Experimental and Numerical Study

compaction frame was removed by detaching raft and the raft was reconnected with the piles such that it flushes with the levelled surface of the sand bed (Figure 4-38). The density of sand was checked by using rigid wooden boxes as discussed earlier at different elevation within the tank. In case of only pile/pile group, small cap/raft was kept 5 cm above the sand bed (Figure 4-37).

3. The proving- ring for measuring load on the raft/piled raft was placed in the centre of the model, so that it coincided with the centre of the mechanical screw jack. A small metal ball was kept between the proving ring and the mechanical screw jack so that the model could be subjected to concentric load. To calculate the settlement due to applied load, four dial gauges / LVDTs with sensitivity of 0.01 mm were placed at the four corners of the raft.

4. The maintained load test (MLT) method was used for all tests, and the load increment was kept at $1/8^{\text{th}}$ to $1/10^{\text{th}}$ of the estimated ultimate capacity of a unpiled raft/piled raft as the case may be. The load increment was held until the rate of settlement becomes negligible 0.01 mm per 5minutes or minimum 1 hour. The procedure was repeated until the progressive large settlement was reached or failure was noticed.

5. When the readings were stabilised, the settlement and EPC readings were taken for each load increment.

Experimental and Numerical Study

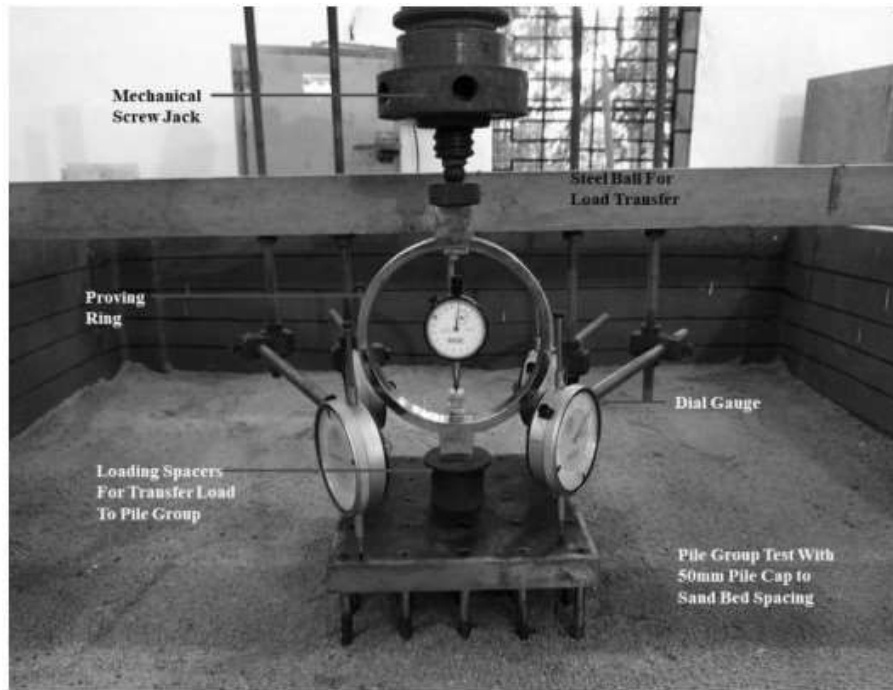


Figure 4-37 : Experimental setup for load test on pile group



Figure 4-38 : Experimental setup for load test on piled raft

Experimental and Numerical Study

4.2 Numerical Study

4.2.1 General

For the analysis of piled raft foundation Plaxis 3D version 2023.1.0 by Bentley Systems was used.

The first step of the modeling process is to define the model boundaries. Pile, raft, and soil are the main components of piled raft which should be modeled. The model boundaries were selected to avoid any influence of the outer boundaries. To eliminate boundaries effect, the lateral boundaries of the model were set at a distance equal to 2.5 times the raft width measured from the centre of the raft. The depth of the model was 2 times maximum length of pile. The mechanical behaviour of soil may be modeled at various degrees of accuracy. PLAXIS includes various types of constitutive models to simulate the behaviour of materials. The elastic-perfectly plastic Mohr-Coulomb (MC) model was used to simulate the behaviour of the soil. The soil was considered as Mohr-Coulomb model and the various properties of soil are mentioned in Table 4-7. The Elastic Modulus of soil was calculated with triaxial test results data which was performed on the Orsang river sand at 40%, 60% and 80% relative density. Modulus of elasticity of sand E_s was taken an average of three slopes of the initial tangent of deviator stress-strain curve at different cell pressures. Young's modulus E_{50} was obtained from the initial stage of the stress-strain curve measured in triaxial tests. It is evaluated as a secant stiffness for the interval between deviator stress $\sigma_d = 0$ and $\sigma_d = \sigma_{d, max}/2$ (Wichtmanni et al., 2017). It is vital to enter precise values that are typical of the particular materials being examined when establishing the poisson's ratio (μ) in PLAXIS 3D. The values of Poisson's ratio normally fall between 0 and 0.5, where 0 denotes an entirely incompressible material and 0.5 denotes an expandable material without axial strain. The values of μ are calculated using the formula (4-2) (Federico, 2009).

$$\mu = \frac{1 - \sin\phi}{2 + \sin\phi} \quad (4-2)$$

Where, ϕ = angle of internal friction

Experimental and Numerical Study

R_{inter} is an interaction factor used in pile-soil interaction models to measure the extent of load transmission from a pile to the surrounding soil through shaft resistance. It determines the load distribution and pile-soil interaction behaviour. The value of R_{inter} depends on soil characteristics, pile geometry, and applied load, and can be determined through empirical relationships or calibration with field tests. R_{inter} ranges from 0 (no interaction) to 1 (complete interaction). R_{inter} values used in design are mentioned in Table 4-8.

The interaction of soil with concrete was taken as 0.67 (Martirosyan, 2019). A composition of finite elements is called a mesh. The mesh should be sufficiently fine to obtain accurate numerical results. On the other hand, the increase in mesh density leads to excessive calculation times. PLAXIS 3D uses fully automatic generation of finite element meshes. Medium meshing is selected for the present numerical model. Interface elements in PLAXIS 3D are used to model the interaction between different materials or interfaces. They enable the transfer of forces and deformations across the interface, capturing non-linear behaviour and interaction between neighboring materials. These elements consider properties like shear resistance, normal stiffness, and dilatation. With appropriate boundary conditions, they accurately simulate soil-structure interaction. During analysis, the behaviour of interface elements is incorporated into the equations. Post-processing provides visualizations of shear stresses, normal stresses, contact pressures, and interface displacements. In the present work, two types of interfaces were given one positive interface between raft and point load and second a negative interface between raft and soil.

The pile was modelled as an embedded beam element. The base resistance and skin resistance were determined using IS: 2911 (part 1/Sec 2): 2010 for cohesion less soil.

For the present study, raft was considered as volume element and as linear-elastic material and drainage material was considered as non- porous.

For the model piled-raft, the load was taken in the increment 1.328 kN. Load settlement data was obtained at a point below point load and at the centroid of the shape of raft, and the load shared by pile was taken as maximum axial force taken at each pile (Figure 4-39).

Experimental and Numerical Study

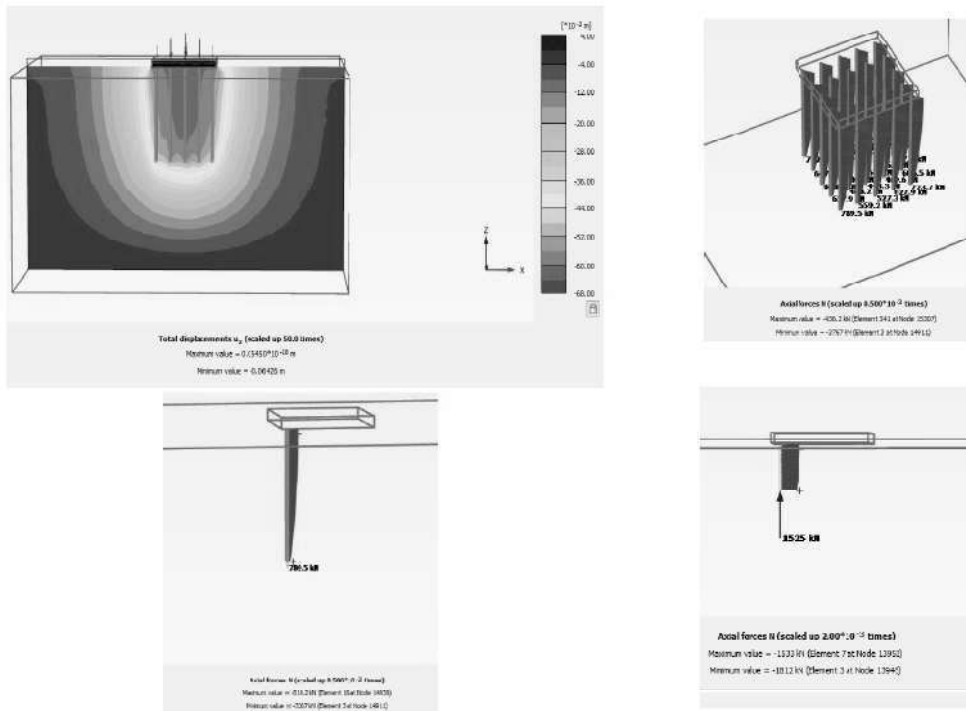


Figure 4-39 : Output of the numerical analysis

Table 4-7 properties of soil

| Parameter | Value | | |
|---|------------|----------|---------|
| Maximum density (kN/m ³) | 1.83 | | |
| Minimum density (kN/m ³) | 1.5 | | |
| e _{max} | 0.7 | | |
| e _{min} | 0.39 | | |
| Relative density I_d (%) | 40 | 60 | 80 |
| Soil density (kN/m ³) | 16.16 | 16.8 | 17.5 |
| Modulus of elasticity of sand E_s (kPa) | 21667 | 33889 | 39167 |
| Young's modulus E_{50} (kPa) | 12181.7432 | 17539.83 | 11546.8 |
| Angle of internal friction (ϕ) | 32 | 35 | 39 |
| ϕ_{inter} | 22.55 | 24.5 | 26.3 |
| R_{inter} | 0.66 | 0.65 | 0.6103 |
| Poisson ratio (μ) | 0.319 | 0.298 | 0.27 |

Experimental and Numerical Study

Table 4-8 Properties of soil used for defining soil model (for validation of experimental study and prototype analysis)

| Parameter | Value |
|---|----------|
| Maximum density (kN/m ³) | 1.83 |
| Minimum density (kN/m ³) | 1.5 |
| e_{\max} | 0.7 |
| e_{\min} | 0.39 |
| Relative density I_d (%) | 60 |
| Soil density (kN/m ³) | 16.8 |
| Modulus of elasticity of sand E_s (kPa) | 33889 |
| Young's modulus E_{50} (kPa) | 17539.83 |
| Friction Angle (ϕ) | 35 |
| ϕ_{inter} | 24.5 |
| R_{inter} | 0.65 |
| Poisson Ratio (μ) | 0.298 |

Table 4-9 Properties of model mild steel Pile (for validation of experimental study)

| Parameter | Value |
|----------------------------------|-------------------|
| Unit Weight (kN/m ³) | 78.5 |
| Elastic Modulus (kPa) | 200×10^8 |
| Poisson's Ratio | 0.28 |
| Diameter of pile (d) (mm) | 9.7 |
| Pile Length L (mm) | $10d, 20d, 30d$ |

Table 4-10 Properties of Raft (for validation of experimental study)

| Parameter | Value |
|----------------------------------|-------------------|
| Unit Weight (kN/m ³) | 78.5 |
| Elastic Modulus (kPa) | 200×10^8 |
| Poisson Ratio (μ) | 0.28 |

Experimental and Numerical Study

4.2.2 Validation of Numerical Model

4.2.2.1 Validation with Numerical Analysis

Validation is necessary to justify numerical model predictions and ensure accurate modeling. To validate the results of the developed model (PLAXIS 3-D model), three examples of piled-raft foundations were taken. First example of Messe-Torhaus Building was presented by Engine et al. (2009) from Delft University of Technology, Delft, Netherlands was analyzed. Second example was taken from the research paper of Ahmed et al. (2021). Third example was taken from the research work of André Ryltenius (2011).

1) Messe-Torhaus Building Piled Raft Case

The 130 m Messe-Torhaus building in Frankfurt, constructed between 1983 and 1986, was a pioneering structure in Germany with a piled-raft foundation design (Figure 4-40). The foundation system consisted of 84 bored piles, each 20 m in length and 0.9 m in diameter, supporting two large rafts measuring 17.5 m × 24.5 m. The distance between the two rafts was 10 m.

The bottom of the 2.5 m thick raft was positioned 3 m below ground level. The subsurface soil profile beneath the rafts consisted of quaternary sand and gravel up to a depth of 2.5 m, followed by the Frankfurt clay. The groundwater level was located below the rafts. To monitor the geotechnical behaviour of the piled-raft foundation, six instrumented piles, eleven contact pressure cells, and three multi-point borehole extensometers were employed. The positions of these measurement devices are illustrated in Figure 4-40.

The design of the piled-raft foundation followed a conventional approach, assuming that the piles would be loaded to their ultimate bearing capacities, while the raft would transmit the remaining load (Katzenbach et al., 2000). To validate the behaviour of the embedded piles in a group configuration, Plaxis 3D Foundation software was utilized to model this specific case and uniformly distributed surface load was applied on the raft of left side.

Experimental and Numerical Study

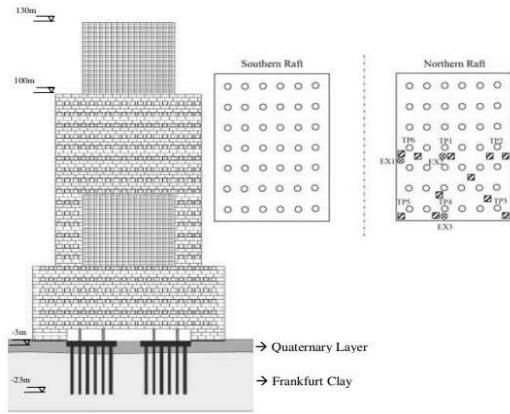


Figure 4-40 : Messe - Torhas Building

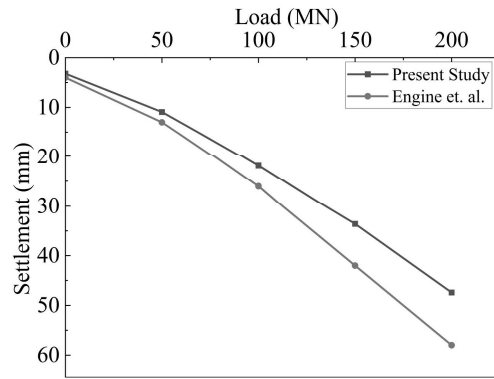


Figure 4-41 : Validation of the present numerical model with numerical results reported by Engine et.al (2009)

The soil parameters used in the finite element analysis are given in Table 4-11. For the raft a unit weight, $\gamma_{raft} = 25$ kN/m³, a Young's modulus, $E = 3.7 \times 10^7$ kN/m² and a Poisson's ratio, $\mu = 0.2$ is used. A reduced stiffness was used during raft installation to ensure a proper transfer of the raft load on to the underlain soil. Embedded pile properties are given in

Table 4-12. All piles are given the same pile resistances (tip and skin).

The load settlement characteristic of piled raft for this case obtained from present model was compared with the obtained by Engine et al. (2009) as shown in Figure 4-41.

Table 4-11 Properties of soil (Messe - Torhas Building)

| Property | unit | Quaternary sand and gravel | Frankfurt clay |
|--|-------------------|----------------------------|-------------------|
| Unit weights, γ' / γ_d | kN/m ³ | 11/19 | 10/20 |
| Secant stiffness, E_{50} | kN/m ² | 3.0×10^4 | 3.5×10^4 |
| Cohesion | kN/m ² | 0.0001 | 20 |
| Angle of internal friction | degree | 35 | 20 |
| K_0 | - | 0.426 | 0.8 |
| Interface stiffness ratio, R_{inter} | - | 1 | 1 |

Experimental and Numerical Study

Table 4-12 Properties of pile (Messe - Torhas Building)

| Property | unit | Value |
|----------------------------|-------------------|-------|
| Pile diameter, D | m | 0.9 |
| Pile length, L | m | 20 |
| Unit weight, γ | kN/m ³ | 15 |
| Poisson's ratio, μ | - | 0.2 |
| Young's modulus, E | - | 0.426 |
| T_{\max}^{top} | kN/m | 453 |
| T_{\max}^{bottom} | kN/m | 453 |
| Max. tip resistance | kN | 1200 |

2) Settlement Performance of Piled Raft Foundations in Sand (Ahmed et al. (2021))

A comprehensive study was conducted to analyze the load-settlement behaviour of a piled raft foundation resting on sandy soil. The research aimed to investigate the influence of key parameters on the foundation's performance. The subsoil consisted of homogeneous dry medium sand with a dry density (D_r) of 65%, and its properties, as reported by Elwakil and Azzam, were used in the analysis (Table 4-13). The raft and piles were constructed using concrete, and the soil behaviour was simulated using the elastic-perfectly plastic Mohr-Coulomb model, while the raft and pile elements were modeled with a linear elastic model. Material properties relevant to the finite element analysis are summarized in a Table 4-13. The parameters considered in this study were the length of the piles (L_p), the diameter of the piles (d_p), the thickness of the raft (t_r), and the internal friction angle of the sand soil (ϕ). A range of typical values for these parameters was selected for the analysis (Table 4-13).

The numerical models consisted of a square raft with plan dimensions of 4.0 m \times 4.0 m, supported by four piles spaced at a distance of 5 times the pile diameter ($5d_p$). The analyses were performed on various piled raft models subjected to a vertical uniformly distributed load of 200 kPa.

Experimental and Numerical Study

Table 4-13 Material properties used in numerical analysis (Ahmed et al. (2021))

| Parameter | Sand | Raft & Pile |
|---|---------------|------------------------|
| Material Model | Mohr- Coulomb | Linear Elastic |
| Drainage Type | Drained | Drained |
| Unit weight (kN/m ³) | 18 | 25 |
| Poisson's Ratio | 0.3 | 0.15 |
| Youngs's modulus (kN/m ²) | 5000 | 22 ×10 ⁶ |
| Effective Cohesion (kN/m ²) | 0.1 | - |
| Angle of Internal Friction | 35 | - |
| Angle of Dilatancy | 5 | - |
| Interface Strength Reduction | 0.67 | - |

The analysis of the piled raft foundations involved three stages: the initial stage, construction stage, and loading stage. In the initial stage, the soil domain was activated. The construction stage involved activating the raft and piles. Finally, in the loading stage, the applied load was activated to assess the load-settlement behaviour of the piled raft foundation. The load-settlement behaviour obtained by running the present model and obtained by Ahmed et al. (2021) shows good agreement with each other as shown in Figure 4-42.

Experimental and Numerical Study

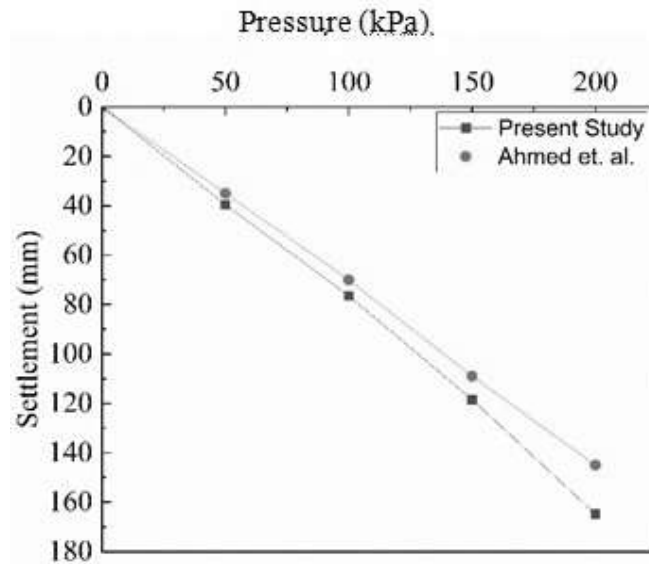


Figure 4-42 : Comparison of Load –settlement characteristic obtained from present study with Ahmed et al. (2021)

3) Piled raft foundation in Plaxis 3D (ANDRÉ RYLTIENIUS)

The geometry of the piled raft is illustrated in Figure 4-43. The piled raft is situated on a single layer of soft clay and supports a uniform load of 30 kN/m^3 . The piles are chosen to SP3 piles (Swedish standard), which are square pre-cast concrete piles with the width of 275 mm. The raft and the piles were assumed to have a Young's modulus of 35 GPa. The firm rock is situated 40 m below the ground surface and the ground water table is situated three meters below the ground surface.

The model is $160 \text{ m} \times 160 \text{ m} \times 40 \text{ m}$, thus the same width as the plane strain model. A borehole was defined, which is 40 meter deep and with the water level situated 3 meters below the ground surface. The bore hole was assigned the material properties (clay).

Experimental and Numerical Study

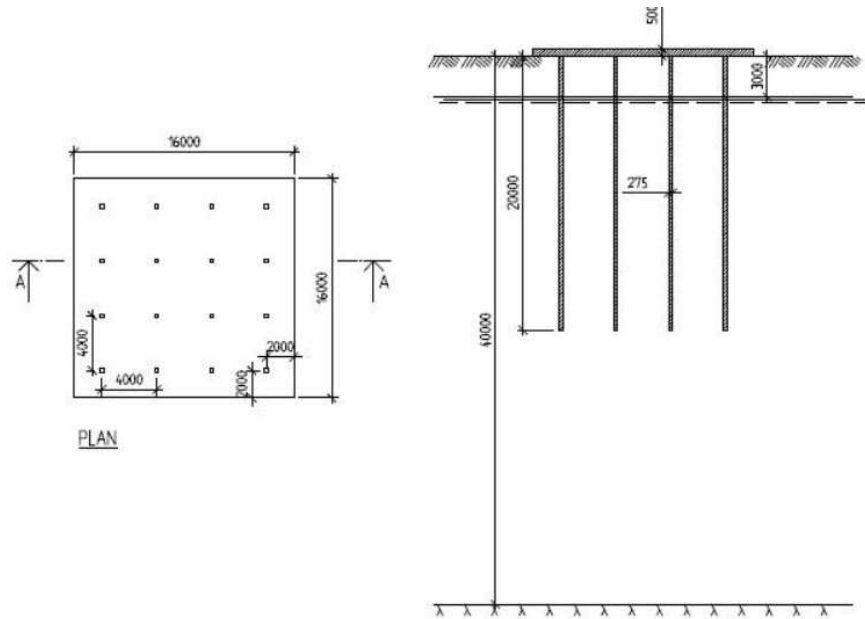


Figure 4-43 : Piled raft profile (after ANDRÉ RYLTIENIUS)

Table 4-14 Material parameters for the soil (ANDRÉ RYLTIENIUS)

| Input parameter of clay | unit | Value |
|----------------------------|-------------------|-------|
| Young's module | kN/m ² | 5000 |
| Poisson's ratio | - | 0.35 |
| Saturated unit weight | kN/m ³ | 18 |
| Unsaturated unit weight | kN/m ³ | 18 |
| Cohesion | kN/m ² | 4 |
| Friction angle | degrees | 30 |
| Dilatancy angle | degrees | 0 |
| Interface reduction factor | - | 0.8 |

Table 4-15 Material parameters for the raft (ANDRÉ RYLTIENIUS)

| Input parameter of raft | unit | Value |
|-------------------------|-------------------|----------------------|
| Young's module, | kPa | 35 x 10 ⁶ |
| Poisson's ratio, | - | 0.2 |
| Unit weight | kN/m ³ | 25 |
| Height | m | 0.5 |

Experimental and Numerical Study

Table 4-16 Material parameters for the embedded piles (ANDRÉ RYLTIENIUS)

| Input parameter of pile | unit | Value |
|-------------------------|-----------------|------------------|
| Young's module, | kPa | 35×10^6 |
| Unit weight | kN/m^3 | 25 |
| Width | m | 0.275 |

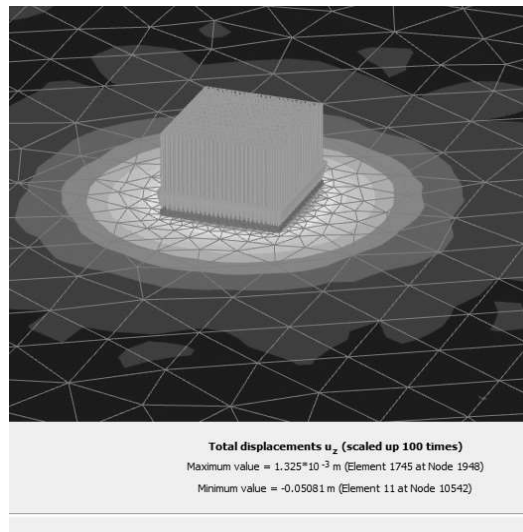


Figure 4-44 : Total displacement for the study

The displacement obtained by author was 56 mm, while in the present work it was found to be 51 mm which is quite close to the 56 mm (Figure 4-44).

4.2.2.2 Validation with Experimental Result

The validation of numerical model was also done by comparing the load-settlement characteristics of piled raft obtained from the present experimental study for following two cases.

- 1) square piled raft with 9 piles in square group: L/d ratio of pile = 30; spacing between piles = $7d$; $I_d = 60\%$

Experimental and Numerical Study

- 2) square piled raft with 25 piles in square group: L/d ratio of pile = 20; spacing between piles = $5d$; $I_d = 60\%$

Table 4-17 Parametric details of pile, raft, and piled raft foundation used in the experimental study for the Validation of the present numerical model

| Test No. | Parametric Details | | | | | |
|----------|--------------------|----------|----------|----------|------------------------------|------------|
| | d_i (mm) | d (mm) | S (mm) | L (mm) | Raft size (mm ³) | Pile group |
| 1 | 7.8 | 9.7 | 67.9 | 291 | 220 × 220 × 25 | 3 × 3 |
| 2 | 7.8 | 9.7 | 48.5 | 194 | 220 × 220 × 25 | 5 × 5 |

d_i = internal diameter of pile; d = outer diameter of pile; S = spacing between piles; L = embedded length of pile

The results obtained from Plaxis 3D and experimental study were compared as shown in Figure 4-45 and Figure 4-46.

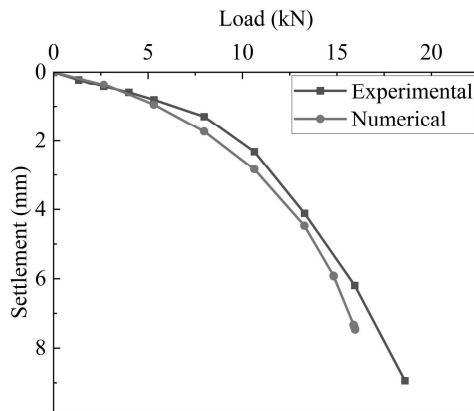


Figure 4-45 : comparison of load settlement characteristics of model piled raft from experimental and numerical study (Square piled raft with 9 piles in Square group: L/d ratio of pile = 30; spacing between piles = $7d$; $I_d = 60\%$)

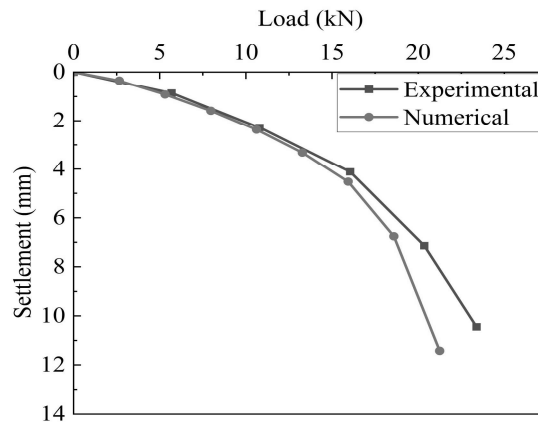


Figure 4-46 : comparison of load settlement characteristics of model piled raft from experimental and numerical study (Square piled raft with 25 piles in Square group: L/d ratio of pile = 20; spacing between piles = $5d$; $I_d = 60\%$)

The results obtained were found near to experimental results and the difference was found nearly 10 and less than 10% in both cases.

Experimental and Numerical Study

4.2.3 Prototype Piled- Raft Foundation

To know the effect of various configuration of pile with actual PRF in the field, a numerical study was conducted for the same. The model geometry consisted of square raft $13.608 \text{ m} \times 13.608 \text{ m} \times 1.5 \text{ m}$ were used to simulate the rigid rafts. The raft-soil stiffness ratio ($K_{rs} > > 5$), confirm the rigidity of the raft. The raft was taken as volume element resting on ground surface with an interface provided between the raft and the underlying soil. The pile was taken as embedded beam, whereas Mohr-Coulomb model was considered for the soil and the mesh considered was medium. The properties of soil, raft, and pile are given in Table 4-8 & Table 4-18. R_{inter} value in soil was taken as 0.67 (Armen 2019).

The area of soil profile taken into consideration is $5B_r$ in horizontal direction and $2B_r$ depth. Variation in L/d (length of pile (L) to diameter of pile (d) ratio) of piles in different configuration and pattern were considered in the analysis. The total number of piles (n_p) and spacing (s_p) between the piles was kept constant in all cases. Piles are considered with diameter of 0.6 m and length varying as $10d$, $20d$ and $30d$. The various configurations of piles considered are given in Figure 4-47. The spacing between piles was considered as $5d$ along length and breadth in case of square pattern whereas as in case of circular pattern the spacing was considered as $5d$ in radial direction.

Table 4-18 Properties of Pile and Raft considered in the study

| Parameter | Value |
|--|-----------------------------------|
| Unit Weight of raft and pile (kN/m^3) | 25 |
| Elastic Modulus (kPa) | 30×10^8 |
| Poisson's Ratio (ν) | 0.2 |
| Size of square Raft (m^3) | $13.608 \times 13.608 \times 1.5$ |
| Diameter of pile d (m) | 0.6 |
| Pile Length (m) | $10d, 20d, 30d$ |

Experimental and Numerical Study

Table 4-19 Details of configurations

| Configuration pattern | Numbers of Long Piles | Numbers of Medium Piles | Numbers of Short Piles |
|-----------------------|-------------------------|-------------------------|-------------------------|
| | (<i>L/d ratio=30</i>) | (<i>L/d ratio=20</i>) | (<i>L/d ratio=10</i>) |
| <i>S1;C1</i> | 16 | 8 | 1 |
| <i>S1;C1</i> | 1 | 8 | 16 |
| <i>S1;C1</i> | 9 | 0 | 16 |
| <i>S1;C1</i> | 16 | 0 | 9 |
| <i>S1;C1</i> | 9 | 12 | 4 |
| <i>S1;C1</i> | 4 | 12 | 9 |
| <i>S1;C1</i> | 0 | 0 | 25 |
| <i>S1;C1</i> | 0 | 25 | 0 |
| <i>S1;C1</i> | 25 | 0 | 0 |

- **CONFIGURATION OF PILE**

Two types of configurations pattern were used in study i.e. square and circular with varying length of pile as shown in Figure 4-47. Various configurations of the pile in square pattern were denoted by *S1 to S9* and circular pattern by *C1 to C9*.

Experimental and Numerical Study

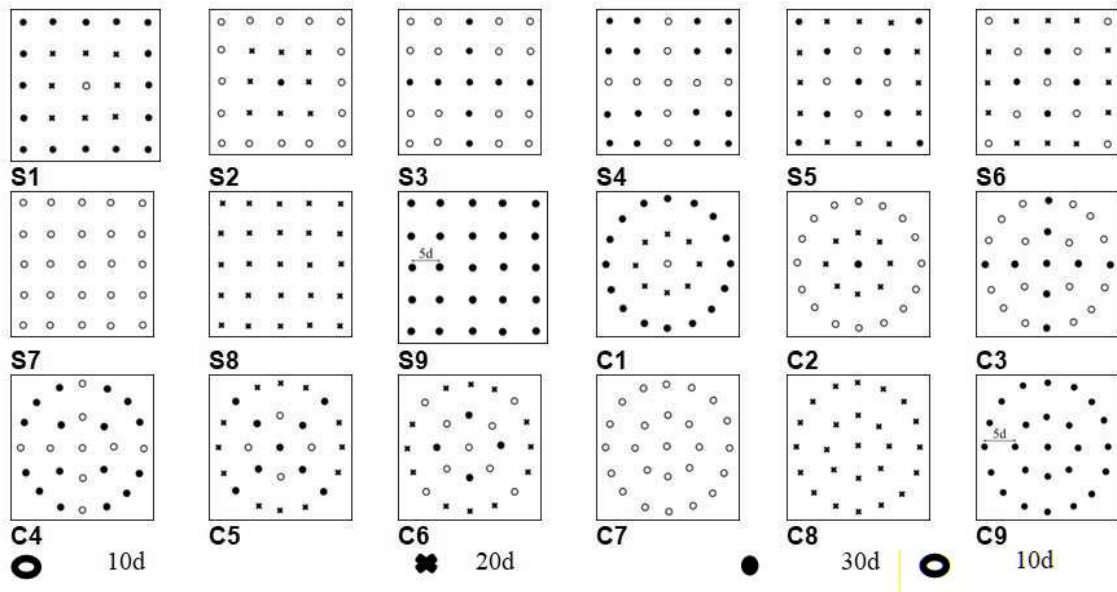


Figure 4-47 : Various Configuration of pile in square pattern (S1 – S9) and circular pattern (C1- C9)

Application of Load on Piled Raft

Three loads P1, P2 and P3 were considered as column loads at 9 locations as shown in Figure 4-48 such that P1: P2: P3 is in the ratio of 3:2:1, with maximum load (P1) at the centre. Load was increased at same ratio for determining the load settlement curve and for determining various results. The base resistance and skin resistance of the pile was calculated using IS 2911.

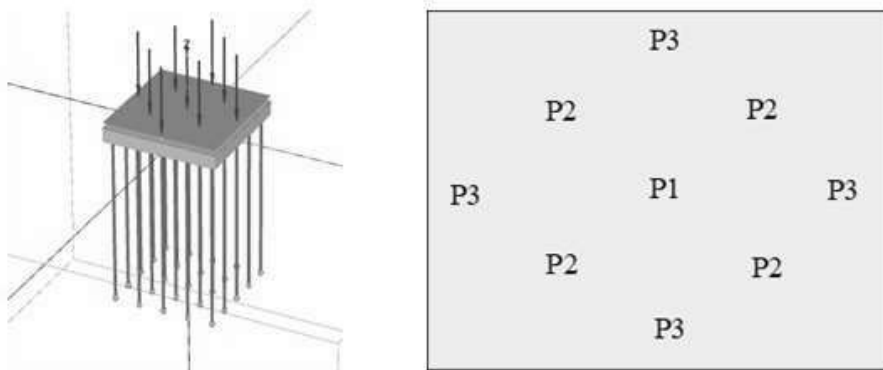


Figure 4-48 : Load considered in the large piled raft